Dept. of Mech. Eng.
CUET

Published Online March 2015 (http://www.cuet.ac.bd/merj/index.html)

Mechanical Engineering Research Journal

Vol. 9, pp. 1–6, 2013

ISSN: 1990-5491

A SINGLE AIR BUBBLE RISE IN WATER: A CFD STUDY

M. T. Islam[1*], P. Ganesan[1], J. N. Sahu[2], M. N. Uddin[2] and A. Mannan[3]

[1]Department of Mechanical Engineering, University of Malaya, 50603, Kuala Lumpur, Malaysia
[2]Department of Chemical Engineering, University of Malaya, 50603, Kuala Lumpur, Malaysia
[3]Department of Mechanical Engineering, Chittagong University of Engineering & Technology, 4349, Chittagong, Bangladesh

Abstract: In this paper, the combined level set (LS) and volume of fluid (VOF) method has been used to numerically investigate the rising behavior of a single gas bubble through the stagnant liquid in a rectangular domain and trapezoidal domain using CFD code FLUENT. A single air bubble rises into stagnant water has been considered and modeled for three different bubble sizes. A set of transient conversion equations of continuity, momentum, surface tension and gravitational force effects were solved by pressure implicit splitting operator (PISO) algorithm and a piecewise linear interface calculation (PLIC) was applied to solve the movement of gas-liquid interface characteristic. The simulation result of air bubble rise behavior was well agreement with available literature results. It is observed that the bubble velocity is affected by the shape of a column. A higher bubble velocity is found in the rectangular domain than that of the trapezoidal domain.

Keywords: *Computation fluid dynamics (CFD), volume of fluid (VOF), terminal velocity*

NOMENCLATURE

Symbol	Meaning	Unit
V_b	Terminal velocity	(m/s)
d_b	Bubble diameter	(mm)
D_t	Column diameter	(mm)
SF	Scale factor	[-]

1. INTRODUCTION

Gas–liquid bubble columns are commonly used as multi-phase reactors in chemical, biochemical and industrial process, etc., for its advantages such as a high mass and heat transfer and an effective inter-phase contact [1–4]. In bubble column, the motion of bubbles can be very complex due to high density and viscosity ratios. It is also difficult to obtain an accurate mathematical model that can be used to calculate the bubble rise velocity in various physical properties and system parameters. The bubble rise behaviors are strongly depends on a bubble size and gas - liquid properties likes density, viscosity and surface tension [2]. Therefore, it is important to understand the basic knowledge of the complex bubble flow. In recent year, computational fluid dynamics (CFD) with the enhancement of numerical algorithm and computing power, a better physical understanding of two-phase flow problem likes a single bubble rising behavior can be obtained. For example, Mukundakrishnan et al. [5] had done a numerical investigation of an axis-symmetric rise and deformation of spherical gas bubble released from rest in stagnant water. They had shown a significant effect of column wall to the bubble rise velocities and shapes.

The volume of fluid (VOF) method has been used for simulation of the two-phase flow [6]. VOF is a well-known technique for an interface tracking of the motion of all phases, which is included in the governing equation and continuum surface force (CSF) equation at the interface [7–12]. In addition, the level-set (LS) method [8,13,14] is used with a volume of fluid to improve the interface tracking and bubble shapes in the current study.

The purpose of this study is to carry out numerical investigations of three different sizes of gas bubbles rising in water in different shapes of column, i.e., rectangular domain and trapezoidal domain, which is not available in the literature. Results from this study could be useful to understand the true physical phenomena and design of a bubble column reactor.

[*] **Corresponding author:** Email: oly_05me@yahoo.com; Tel: +601128248549

2. MATERIALS AND METHODS

2.1 Materials

In the current study, water is used as the primary phase (liquid) and air is used as secondary phase and the physical properties of the water and the air are shown in Table 1.

Table 1 Physical properties of the liquid and gas in the simulation

Phase	Density (kg/m^3)	Viscosity (Pa.s)	Surface tension (N/m)
Water	998.2	0.001	0.0728
Air	1.225	1.789×10^{-5}	-

2.2 Governing equations

For incompressible flow and a constant density fluid, the continuity and momentum equations are as follows-

$$\nabla.\mathbf{u} = 0 \tag{1}$$

$$\frac{\partial(\rho\mathbf{u})}{\partial t} + \nabla.(\rho\mathbf{u}\mathbf{u}) = -\nabla p + \nabla.\tau + \rho\mathbf{g} + \mathbf{F_b} \tag{2}$$

where $\mathbf{u}$ is the velocity vector, ρ is the density and μ is the viscosity, p is the pressure, $\mathbf{g}$ = (0, −g) is the gravitational acceleration and τ is the stress tensor as follows-

$$\tau = [\mu\{\nabla\mathbf{u} + (\nabla\mathbf{u})^T\}] \tag{3}$$

The dynamic stress balance is realized through the CSF model, which is incorporated in the momentum equation by introducing a volume force $\mathbf{F_b}$ as described by Brackbill et al. [15]. This localized volume force is calculated from the volume fraction data using-

$$\mathbf{F_b} = \sigma k(\mathrm{x})\tilde{\mathbf{n}}\frac{\nabla\tilde{\mathrm{F}}(\mathrm{x})}{[\mathrm{F}]}.\frac{\rho(\mathrm{x})}{[\rho]} \tag{4}$$

where k is the curvature of the interface. The interface characteristic parameters of the outward normal vector $\tilde{n}$ and the curvature k are calculated by-

$$k = -(\nabla.\hat{\boldsymbol{n}}) = \frac{1}{\tilde{\boldsymbol{n}}}\left[\left(\frac{\tilde{\boldsymbol{n}}}{|\tilde{\boldsymbol{n}}|}\cdot\nabla\right)|\tilde{\boldsymbol{n}}| - (\nabla\cdot\tilde{\boldsymbol{n}})\right] \tag{5}$$

$$\tilde{\boldsymbol{n}} = \left(\tilde{n}_x\tilde{n}_y\right);\ \hat{\boldsymbol{n}} = \frac{\tilde{\boldsymbol{n}}}{|\tilde{\boldsymbol{n}}|} \tag{6}$$

The curvature k is given in terms of $\tilde{\boldsymbol{n}}$ and $|\tilde{\boldsymbol{n}}|$ to ensure the main contribution from the finite difference approximation of k comes from the centre of the transition region rather than the edges [15].

In VOF method, the motion of the gas-liquid interface is tracked based on the volume fraction function, F. When F is unity, the space is occupied by the liquid phase, when F is zero, the space is occupied by the gas phase and when F is between 0 and 1, the space contains both the gas and liquid phases. The standard advection equation for F is given by

$$\frac{\partial\mathrm{F}}{\partial t} + \nabla.(\mathbf{u}\mathrm{F}) = 0 \tag{7}$$

The volume tracking algorithms are used to capture the interfaces. In this current study, the Piecewise Linear Interface Construction (PLIC) algorithm [16] is adopted to solve Eq. (7) and to reconstruct the interfaces since it has a high accuracy. The mixture properties used in Eq. (2) can be defined by-

$$\rho(\mathrm{F}) = \mathrm{F}\rho_l + (1-\mathrm{F})\rho_\mathrm{g} \tag{8}$$

$$\mu(\mathrm{F}) = \mathrm{F}\mu_l + (1-\mathrm{F})\mu_\mathrm{g} \tag{9}$$

The level set method [17,18] is used with VOF method for the current study is the level set. The level set function $\varphi(r,\ t)$ is defined by-

$$\varphi(r,t) = \begin{cases} +d & \text{in liquid region} \\ 0 & \text{at interface} \\ -d & \text{in gas region} \end{cases} \tag{10}$$

where d is the shortest distance of a point r from the interface at time t. And the level set equation is given-

$$\frac{\partial\varphi}{\partial t} + \mathbf{u}\cdot\nabla\varphi = 0 \tag{11}$$

Therefore, Eq. 2 can be written as-

$$\rho(\tilde{\alpha})\left\{\frac{\partial\mathbf{u}}{\partial t} + \nabla.(\mathbf{u}\mathbf{u})\right\} = -\nabla p + \rho(\tilde{\alpha})\mathbf{g} + \nabla.\tau + \sigma k\nabla\tilde{\alpha} \tag{12}$$

$$\tau = [\mu(\tilde{\alpha})\{\nabla\mathrm{u} + (\nabla\mathrm{u})^T\}] \tag{13}$$

where $\tilde{\alpha}$ is the smoothed void fraction and $\sigma\ is$ represents the surface tension. The smoothed void fraction field in the CLSVOF method is defined using a smoothed Heaviside function $H_\varepsilon(\varphi)$, defined as-

$$\tilde{\alpha} = H_\varepsilon(\varphi) = \begin{cases} 1 & if\varphi > \varepsilon \\ \frac{1}{2} + \frac{\varphi}{2\varepsilon} + \frac{1}{2\pi}\left[\sin\frac{\pi\varphi}{\varepsilon}\right] & if|\varphi| \le \varepsilon \\ 0 & if\varphi < -\varepsilon \end{cases} \tag{14}$$

Since the density and viscosity of each fluid is constant as the fluid is assumed incompressible, they take two different values as follows-

$$\rho(\varphi) = \rho_l H(\varphi) + [1-H(\varphi)]\rho_\mathrm{g} \tag{15}$$

$$\mu(\varphi) = \mu_l H(\varphi) + [1-H(\varphi)]\mu_\mathrm{g} \tag{16}$$

Where H (φ) is the Heaviside function given by

$$H(\varphi) = \begin{cases} 1 & if\varphi > 0 \\ \frac{1}{2} & if\varphi = 0 \\ 0 & if\varphi < 0 \end{cases} \tag{17}$$

2.3 Geometry

Two dimensional (2D) domain is used to study the flow of a single bubble in a column. The column basically has a height of 100 mm and a width of 50 mm to form a rectangular domain. The width of the top wall is reduced to form a trapezoid domain which shown in Fig. 1. At initial stage of a simulation, an air bubble is imposed at the centre and 10 mm height from the bottom of the domain. In this study, three bubble sizes of 3 mm, 4 mm and 5 mm diameter is studied. The bubble in a quiescent

liquid will rise under the action of the buoyancy force and the bubble rising velocity and its characteristics were numerically investigated.

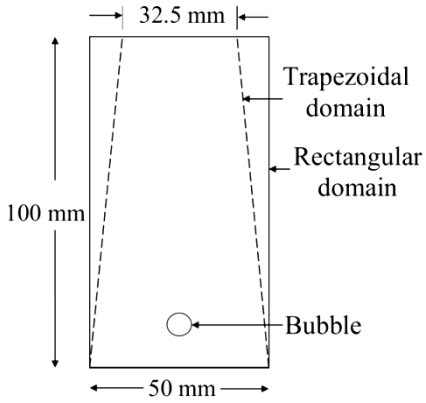

Fig. 1: Computational domain of rectangular domain and trapezoidal domain.

2.4 Boundary condition and numerical methods

The side and bottom walls of the domain are assigned as no slip boundary condition and the top wall as pressure outlet boundary condition. The operating pressure is set to be equal to the ambient pressure, i.e., 101325 Pa and the gravitational force (g) of 9.81 m/s^2 is assigned along –Y direction.

The continuity, momentum and volume of fluid fraction equations were solved using the ANSYS-FLUENT, which is based on the finite volume method [19]. The second order upwind scheme was used for the flow equations [20]. The pressure implicit with splitting operators (PISO) algorithm was applied to solve the pressure-velocity coupling [21], which allows a rapid convergence rate without a significant loss of solution stability and accuracy [20]. Pressure was solved using a body force weighted scheme and an implicit body force treatment was applied to improve the solution convergence. The transient model based on an explicit scheme with a time step of 0.0001s is used which gives a Courant number of 0.25.

2.3 Mesh dependency test

The effect of a mesh size on the results was investigated using three types of meshes in the rectangular domain. The dimensions of each cell in these meshes are 0.20 mm × 0.20 mm, 0.25 mm × 0.25 mm, 0.30 mm × 0.30 mm respectively. A structured mesh as shown in Fig. 2 is used.

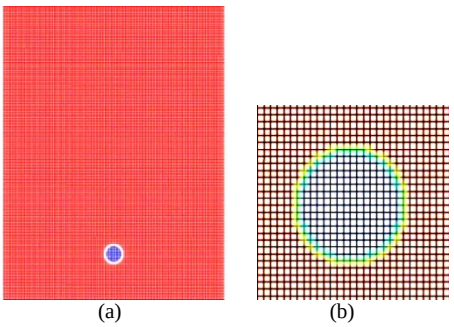

Fig. 2: (a) Physical model of single bubble rising process for 0.25mm × 0.25mm mesh size; (b) Zoom view on mesh around the bubble.

The bubble rising distance with the increase of time in second is shown in Fig. 3 for the different meshes. The results from the mesh with the cell size of 0.20 mm × 0.20 mm are almost the same as that from the cell size of 0.25 mm × 0.25 mm. The results from 0.30 mm × 0.30 mm mesh size slightly differ from that of other meshes especially beyond 0.2 s. The results mean that the optimum accuracy can be reached with 0.30 mm × 0.30 mm mesh size. The less dense mesh of 0.25 mm × 0.25 mm is selected based on the accurate results to reduce computational requirements.

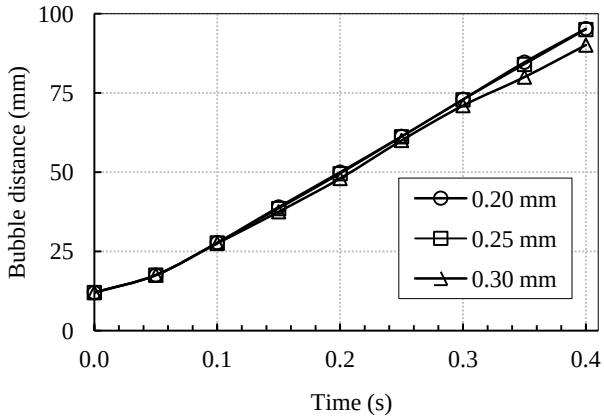

Fig. 3: Mesh dependency test for different types of mesh based on 4 mm bubble diameter in rectangular domain.

3. RESULTS AND DISCUSSION

3.1 Validation of CFD model

Fig. 4(a) shows the rising velocity of a bubble as a function of time for the rectangular column. The results of CFD models checked against the numerical and experimental results of Ma et al. [8] for 4 mm bubble diameter. The results are quite consistent to each other with small differences.

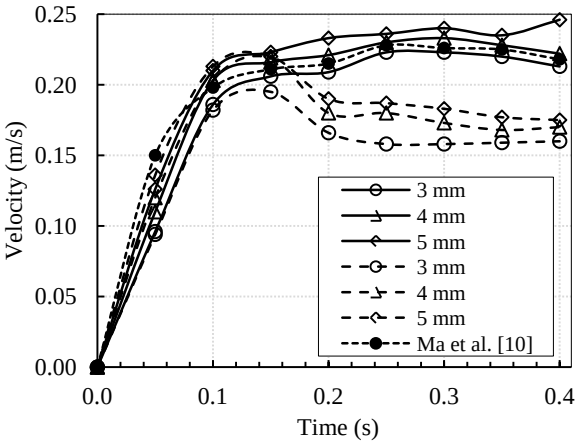

Fig. 4(a): Bubble rising velocities versus time for different bubble size in the rectangular domain (Solid line) and trapezoidal domain (Dash line). Such data from Ma et al. [10] is also included (Dot line) for 4 mm size of bubble.

The terminal velocity from our CFD models are also compared with that obtained using Mendelson equation and Clift et al., which is found in Krishna et al. [22] and the equation was given

as $V_b = SF \times (2\sigma/\rho_l d_b + g d_b/2)^{1/2}$, where $SF = [1 - (d_b/D_t)^2]^{3/2}$. The comparison is shown in Table 2 and the differences are less than 5% for 3-5 mm bubble diameters. This suggests that the CFD models are capable of predicting accurate results.

Table 2 Comparisons between simulation results and correlation for different size of bubble [22]

Bubble diameter (mm)	Correlation (m/s)	Simulation (m/s)	Error (%)
3	0.227	0.216	4.84
4	0.233	0.225	3.43
5	0.249	0.236	4.81

3.2 Bubble rising velocity

Fig. 4(a) shows instantaneous velocities of bubbles of 3-5 mm diameters in the rectangular domain and trapezoidal domain with respect to time increase. From the initial condition up to 0.1 s, the velocities of the bubbles have a steep increase to a peak value of 0.22 m/s in the both domains. Following that, the velocities do not change much and remains almost constant around that value in the rectangular domain. However, this is not the case in the trapezoidal domain where the velocity drops from the peak value at 0.15 - 0.18 seconds before settling near 0.18 m/s velocity.

The difference of velocity of each bubble in the two different columns is shown in Fig. 4(b) in percentage. It can be seen that up to 0.15 s, the differences are very small. Following that, the difference increases for all bubble sizes. In general, a larger difference occurs for a larger bubble size and vice versa, which can be clearly seen at time 0.2 - 0.35 s. For example, the difference is about 23% and 28.5% for 3 mm and 5 mm bubble diameters, respectively at 0.35 s. These results show that trapezoidal column have more effect to a bigger bubble and slows down the rising of the bubble.

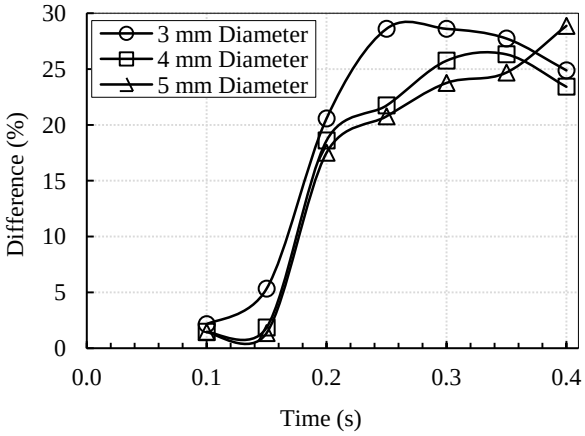

Fig. 4(b): The difference of the bubble rise velocity between rectangular domain and trapezoidal domain for different size of bubble.

Fig. 5(a) shows the bubble rising distance with the increase of time up to 0.4 s for the three bubble sizes in the two different domains. It is observed that up to 0.15 s, there is no significant difference in distance for the bubbles moving up from the initial position of 10 mm to 40 mm in the both domains, which is up to 0.15 s. Following that, the rising distance is not the same for the bubble in the domains. The distance is the highest for 3mm bubble in the rectangular channel and the lowest for 5 mm bubble in the trapezoidal channel.

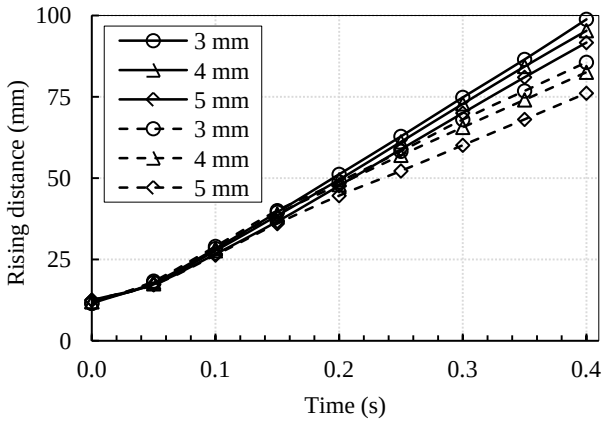

Fig. 5(a): Bubble rising distance at different times for different bubble size in rectangular domain (solid line) and trapezoidal domain (dot line).

Fig. 5(b) shows the percentage difference in distance for the bubbles between the two domains. It is found that from the figure up to 0.15 s, the differences are very small. Following that, the difference increases for all bubble sizes. In general, a larger difference occurs for a larger bubble size and vice versa. For example, the difference is about 13.75% and 17% for 3 mm and 5 mm bubble diameters, respectively at 0.35 s.

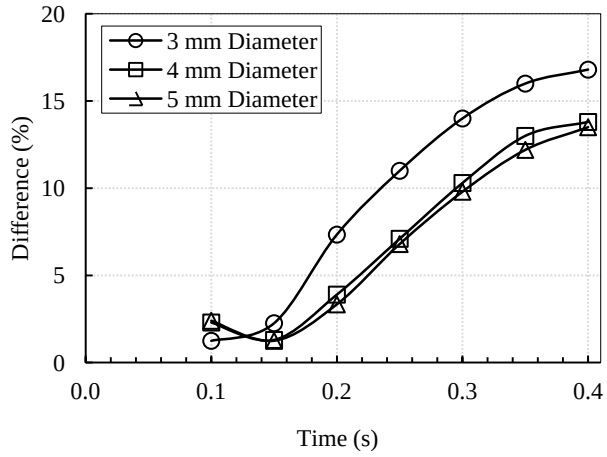

Fig. 5(b): The difference of the bubble rising distance between rectangular domain and trapezoidal domain for different size of bubble.

Fig. 6 shows Weber number (*We*) as a function of Reynolds numbers (*Re*). Weber number is calculated using the equation of $We = (\Delta\rho d_b U_t^2)/\sigma$. The calculation of the Weber number has compared to the correlation of Raymond & Rosant [23], in which *We* is a function of *Re* with the range of Morton number, Mo ~ 9×10^{-7} to 7. The correlation is as followed as $We = 0.42\ Mo^{0.35}\ Re^{(5/3)}$. The results indicate that the *We* increases with the increase of *Re* for both rectangular and trapezoidal domains. Furthermore, around 32% and 47% lower value is found from the correlation result for rectangular and trapezoidal domain, respectively. The plausible reason is that the present work is studied in low Mo ~ 2.8×10^{-11} fluid of water.

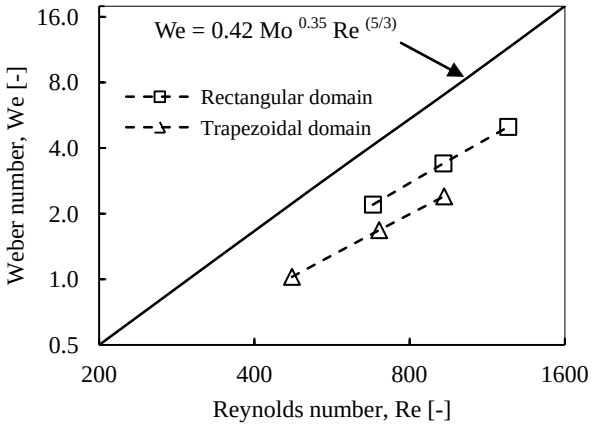

Fig. 6: Weber number as a function of Reynolds number.

3.3 Bubble flow field

In this study, the liquid phase was completely at rest initially due to zero velocity condition. Generally, a single bubble goes to upward due to the buoyancy force and a fluid jet forms at the bottom of the bubble. This jet is pushed the lower surface of the bubble up towards the top surface. The pressure gradient at the lower surface of the bubble is greater than at the top surface of the bubble. Due to this pressure differences, the vortex is forms at the surface with has a rotation and liquid jet that pushes into the bubble from below. The bubble is deformations due to this liquid jet. Generally, the smaller bubbles face less deformation than their larger bubble.

Figs. 7(a) and 7(b) represents the vortices magnitude for 5 mm size of bubble in different domain. As seen from Figures, the bubble rose in upward direction and the maximum vortices was located on the side of the bubble in both rectangular and trapezoidal domain. As seen in Fig. 7(b), secondary vortices were formed due to more deformation of bubble that happened by the shape of the domain as well as effect of wall.

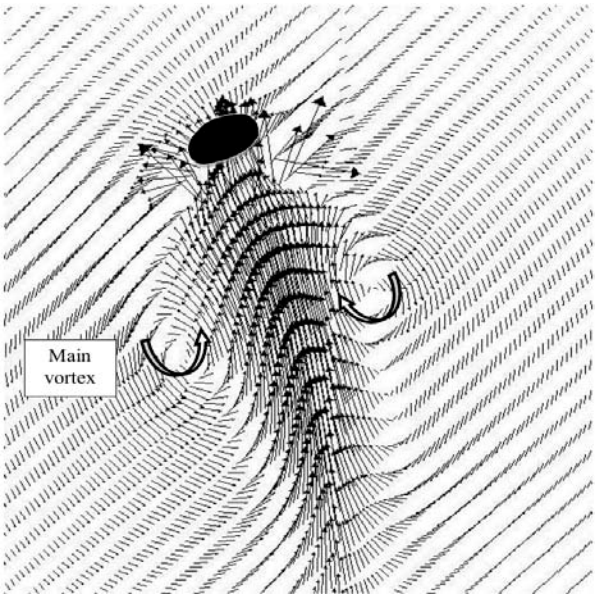

Fig. 7(a): Velocity vectors of 5 mm bubble in rectangular domain at time, t = 0.35 s.

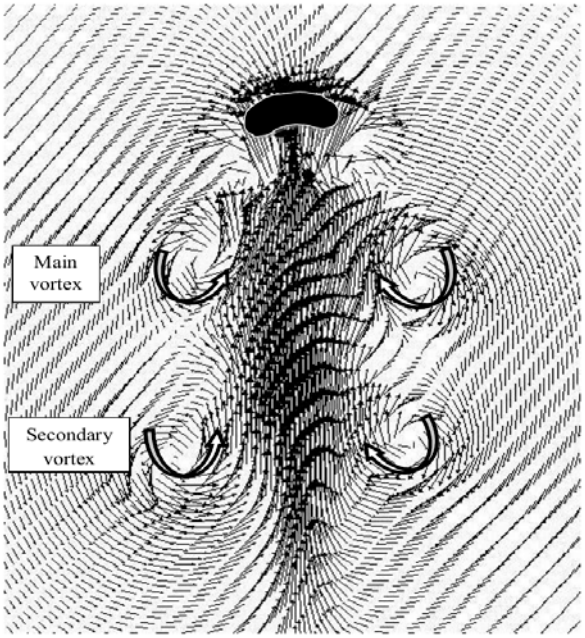

Fig. 7(b): Velocity vectors of 5 mm bubble in trapezoidal domain at time, t = 0.35s.

4. CONCLUSIONS

In this paper, the three different sizes of bubble (i. e., 3 mm, 4 mm and 5 mm) in water in two types of domains have studied numerically using VOF method. The exhaustive conclusions are-

- The bubble velocity from the CFD models is in good agreement with the published papers. This study shows the bubble velocity, which increases with the increase of bubble size and is affected by the shape of a column.
- The bubble velocity is higher in the rectangular domain and lower in the trapezoidal domain. It indicates the effect of wall is apparent in the trapezoidal domain.
- The velocity distribution around the bubble was also investigated. In the trapezoidal domain, the bubble deformation is more due to push of both main and secondary vortex compared to that in the rectangular domain.

5. ACKNOWLEDGEMENTS

The authors are grateful to the University of Malaya (Project No: UM.C/HIR/MOHE/ENG/13) and University of Malaya Research Grant (UMRG: RG121/11AET) for providing the fund for the research work.

REFERENCES

[1] M. Y. Liu and Z. D. Hu, “Studies on the hydrodynamics of chaotic bubbling in a gas-liquid bubble column with a single nozzle”, Chemical Engineering & Technology, Vol. 27, pp. 537–547, 2004.

[2] A. A. Kulkarni and J. B. Joshi, “Bubble formation and bubble rise velocity in gas-liquid systems: a review”,

Industrial & Engineering Chemistry Research, Vol. 44, pp. 5873–5931, 2005.

[3] N. M. S. Hassan, M. M. K. Khan, M. G. Rasul and D. W. Rackemann, "Bubble rise velocity and trajectory in xanthan gum crystal suspension", Applied Rheology, Vol. 20, pp. 65102, 2010.

[4] N. M. S. Hassan, M. M. K. Khan and M. G. Rasul, "Modelling and experimental study of bubble trajectory in non-Newtonian crystal suspension", Fluid Dynamics Research, Vol. 42, pp. 065502, 2010.

[5] K. Mukundakrishnan, S. Quan, D. M. Eckmann and P. S. Ayyaswamy, "Numerical study of wall effects on buoyant gas-bubble rise in a liquid-filled finite cylinder", Physical Review E, Vol. 76, pp. 036308, 2007.

[6] C. W. Hirt and B. D. Nichols, "Volume of fluid (VOF) method for the dynamics of free boundaries", Journal of Computational Physics, Vol. 39, pp. 201–225, 1981.

[7] S. S. Rabha and V. V. Buwa, "Volume-of-fluid (VOF) simulations of rise of single/multiple bubbles in sheared liquids", Chemical Engineering Science, Vol. 65, pp. 527–537, 2010.

[8] I. Chakraborty, G. Biswas and P. Ghoshdastidar, "A coupled level-set and volume-of-fluid method for the buoyant rise of gas bubbles in liquids", International Journal of Heat and Mass Transfer, Vol. 58, pp. 240–259, 2013.

[9] K. Szewc, J. Pozorski and J. P. Minier, "Simulations of single bubbles rising through viscous liquids using smoothed particle hydrodynamics", International Journal of Multiphase Flow, Vol. 50, pp. 98–105, 2013.

[10] D. Ma, M. Liu, Y. Zu and C. Tang, "Two-dimensional volume of fluid simulation studies on single bubble formation and dynamics in bubble columns", Chemical Engineering Science, Vol. 72, pp. 61–77, 2012.

[11] S. Buetehorn, D. Volmering, K. Vossenkaul, T. Wintgens, M. Wessling and T. Melin, "CFD simulation of single-and multi-phase flows through submerged membrane units with irregular fiber arrangement", Journal of Membrane Science, Vol. 384, pp. 184–197, 2011.

[12] N. Yang, Z. Wu, J. Chen, Y. Wang and J. Li, "Multi-scale analysis of gas–liquid interaction and CFD simulation of gas–liquid flow in bubble columns", Chemical Engineering Science, Vol. 66, pp. 3212–3222, 2011.

[13] D. Gerlach, N. Alleborn, V. Buwa and F. Durst, "Numerical simulation of periodic bubble formation at a submerged orifice with constant gas flow rate", Chemical Engineering Science, Vol. 62, pp. 2109–2125, 2007.

[14] K. Yan and D. Che, "A coupled model for simulation of the gas–liquid two-phase flow with complex flow patterns", International Journal of Multiphase Flow, Vol. 36, pp. 333–348, 2007.

[15] J. Brackbill, D. B. Kothe and C. Zemach, "A continuum method for modeling surface tension", Journal of Computational Physics, Vol. 100, pp. 335–354, 1992.

[16] D. Youngs, "Time-dependent multi-material flow with large fluid distortion", Numerical Methods for Fluid Dynamics, Vol. 24, pp. 273–285, 1982.

[17] M. Sussman, A. S. Almgren, J. B. Bell, P. Colella, L. H. Howell and M. L. Welcome, "An adaptive level set approach for incompressible two-phase flows", Journal of Computational Physics, Vol. 148, pp. 81–124, 1999.

[18] H. H. Hariri, Q. Shi and A. Borhan, "Thermo capillary motion of deformable drops at finite Reynolds and Marangoni numbers", Physics of Fluids, Vol. 9, pp. 845, 1997.

[19] A. Fluent, "User's Guide", ANSYS 14.0, 2010.

[20] A. Akhtar, "CFD simulations for continuous flow of bubbles through gas-liquid columns: application of VOF method", Chemical Product and Process Modeling, Vol. 2, pp. 1–19, 2007.

[21] R. I. Issa, "Solution of the implicitly discretised fluid flow equations by operator-splitting", Journal of Computational physics, Vol. 62, pp. 40–65, 1986.

[22] R. Krishna, M. I. Urseanu J. M. van Baten and J. Ellenberger, " Wall effects on the rise of single gas bubbles in liquids", International Communications in Heat and Mass Transfer, Vol. 26, pp. 781–790, 1999.

[23] F. Raymond and J. M. Rosant, "A numerical and experimental study of the terminal velocity and shape of bubbles in viscous liquids", Chemical Engineering Science, Vol. 55, pp. 943–955, 2000.